Time-Resolved Radio Frequency Conductivity (TRRFC) Studies of Charge-Carrier Dynamics in Aqueous Semiconductor Suspensions

Hartmut Herrmann,† Scot T. Martin, and Michael R. Hoffmann*

W. M. Keck Laboratories, California Institute of Technology, Pasadena, California 91125

Received: November 15, 1994; In Final Form: July 25, 1995[⊗]

The time-resolved radio-frequency conductivity (TRRFC) method provides a useful tool for in situ measurements of charge carrier dynamics in aqueous suspensions of semiconductor particles. In this report, the effects of pH on surface states of ZnO and the effects of hole scavengers (2-propanol) are examined. The experimental results are interpreted in terms of surface mediated recombination processes, in which holes are trapped in a fast process by surficial sites on the ZnO. Recombination rates appear to be governed by the reaction rate of electrons with surface-trap sites. At higher pH (i.e., pH 12), electrostatic repulsion due to a negatively charged ZnO surface leads to slower surface recombination rates compared to lower pH (i.e., pH 7) conditions. Addition of a hole scavenger significantly decreases the absolute charge-carrier concentration as detected by TRRFC. This decrease is attributed to the loss of trapped surface holes or surface-bound OH due to oxidation of the hole scavenger. When 2-propanol is used as a solvent, the holes react in a fast step with the solvent at the semiconductor interface within the time resolution of the experiment. The observed TRRFC signal is then due to electrons which are thought to be predominantly transferred to dissolved oxygen (O_2) leading to the formation of hydroperoxyl radicals (HO_2) and subsequently hydrogen peroxide (H_2O_2).

Introduction

Semiconductor particles are used in a wide variety of gas and water treatment technologies.[1−4] In most of these applications, aqueous semiconductor suspensions are employed. However, the investigation of charge-carrier recombination dynamics has been limited to optical methods or time-resolved microwave conductivity (TRMC) techniques that are not easily applicable to aqueous suspensions.[5−9] Spectroscopic methods[10] are normally limited to the study of optically transparent colloidal systems[11] and cannot be applied to opaque disperse systems as often found in water treatment applications (e.g., ZnO or TiO_2 dispersions). Furthermore, the optical techniques currently available do not provide a direct time-resolved measure of conductivity due to the concentration and mobility of holes and electrons generated after irradiation.

Time-resolved radio-frequency conductivity measurements (TRRFC) provide a convenient method for contactless probing of conductivity. TRRFC has been applied in the past for the study of charge carrier dynamics in semiconductors as used in solid-state electronic devices.[5,12−14] In contrast to previous studies we describe a radio frequency conductivity system that allows for the time-dependent study of charge-carrier dynamics in semiconductor particles suspended in water. Our apparatus is utilized to investigate (i) the effects of pH and (ii) the addition of a hole scavenger (2-propanol) on the charge-carrier concentrations within ZnO particles. We believe that this is the first application and report of time-resolved RF conductivity measurements of an aqueous microheterogeneous suspension.

Experimental Section

General Techniques. A schematic of the TRRFC apparatus used in the present study is shown in Figure 1. An excimer laser (Lambda Physik LPX 110 iCC, $\lambda = 308$ nm, typical pulse energy of 75 mJ) irradiates the aqueous sample suspension contained in an NMR tube which is used as the sample cavity. The geometry of the tube allows 40% of the light emitted by the laser to hit the sample. The NMR-tube is centered in a 10-turn coil (length 1.4 cm, diameter $^1/_4$ in. (0.635 cm), 20 gauge copper wire, inductance $L = 240$ nH). The frequency tuning capacitor ranges from 1 to 11 pF and the impedance matching capacitor ranges from 1 to 20 pF. The circuit has a Q value of 40 at zero ionic strength, i.e., Millipore water, 18 MΩ. The entire unit is shielded in an aluminum Faraday cage and is connected to a radio frequency bridge. A Wavetek RF generator (Model 2500-A) drives the bridge at 160 MHz and a maximum output power level of +13 dBm.

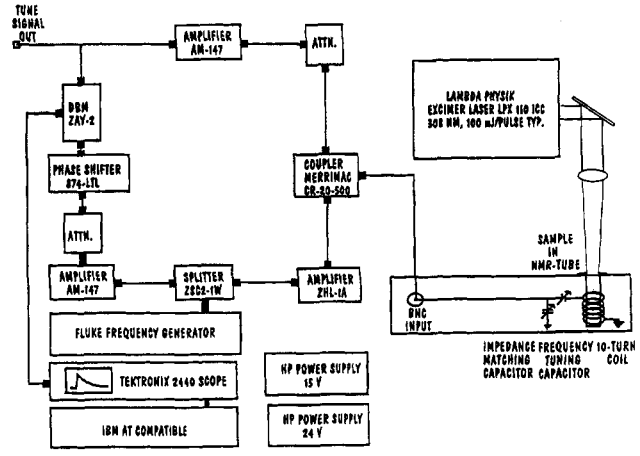

Figure 1. Schematic representation of time-resolved radio frequency conductivity (TRRFC) apparatus.

After samples are placed in the cavity, the RF bridge is tuned to maximize the inductive coupling of the RF bridge and the sample by matching the capacitors in the parallel-series tank circuit. At the resonant frequency only minimum RF power is reflected back to the directional coupler (Merrimac CR-20−500) in the RF circuit so that the detector, a double-balanced mixer (DBM, Mini-Circuits ZAY-2), produces minimum dc

† Universität GH Essen, Institut für Physikalische und Theoretische Chemie, D-45117 Essen, Germany.

* To whom correspondence should be addressed.

⊗ Abstract published in *Advance ACS Abstracts*, September 1, 1995.

0022-3654/95/2099-16641$09.00/0

output. The amplitude of the DBM dc voltage output is proportional to the power reflected from the tank circuit. It is monitored as a function of time by means of a Tektronics storage oscilloscope (Model 2440) and transferred to a computer. The input voltage to the tank circuit is 20 V and the maximum voltage perturbation during an experiment is 0.05%.

Dispersions of ZnO in water (1.0 g/L) were freshly prepared at pH 7.0, 9.5, and 12.0 by the addition of either $HClO_4$ or NaOH to the original dispersion of pH = 7.7. Lower pH's cannot be studied due to the dissolution of ZnO under acidic conditions.[2,3] pH was measured both before and after the experiments (Radiometer Copenhagen PHM 85). pH values were found to be constant within 0.1 pH units. Dispersions were vigorously shaken before each experiment to prevent settling. All chemicals used in the present study were of analytical grade and used without further purification. ZnO powder was obtained from Baker.

Theory of TRRFC Experiment. The dc voltage output of the DBM is sensitive to both the amplitude and the phase of the RF signal reflected back from the sample tank circuit. In principle, changes in both the real and imaginary components of the magnetic permeability, μ, and dielectric constant, ϵ, of the sample circuit affect the reflected signal. The real components of the cited entities are affected by dispersive interaction, whereas the changes in the imaginary components of μ and ϵ are due to absorption. The sample circuit is represented by L and R_2 in the inset of Figure 2a. The microphysical phenomena of eddy currents and resistive heating change L and R_2, respectively. These various descriptions of the experiment are interconnected by the following relationships:

$$L = f(\mu',\epsilon') \rightarrow \text{eddy currents} \tag{1}$$

$$R_2 = f(\mu'',\epsilon'') \rightarrow \text{resistive heating} \tag{2}$$

$$\mu = \mu' + i\mu'' \tag{3}$$

$$\epsilon = \epsilon' + i\epsilon'' \tag{4}$$

Further discussion of the experiment will be in terms of changes in L and R_2.

Equation 5, which describes the typical shape of a Q well (Figure 2a), is derived for the circuit shown in the inset of Figure 2a:

$$\frac{V_{out}}{V_{in}} = \frac{[\alpha^2 R_1^2 \beta + (\alpha^2 R_2(R_1 + R_2) + \beta)^2]^{1/2}}{\alpha^2(R_1 + R_2)^2 + \beta} \tag{5}$$

where $\alpha = \omega C$ and $\beta = (\omega^2 LC - 1)^2$.

Time-dependent changes in the Q well arising from $\Delta L(t)$ following the photogeneration and the subsequent reactions of the charge carriers are shown in Figure 2b. The inset of Figure 2b shows the rise and subsequent decay of the voltage output of the double-balanced mixer (for $\Delta\delta \rightarrow 0$).

The DBM dc voltage output is a function of both the amplitude of the RF signal reflected back from the serial tank circuit and the phase mismatch between the sample and reference signals[15] as follows:

$$V_{DBM} = CV_{ref}V_{out}\cos\delta \tag{6}$$

Because the phase is matched prior to laser irradiation, $\delta(0) = 0$, the change in voltage at the DBM as a function of time, $\Delta V_{DBM}(t)$, is written as follows:

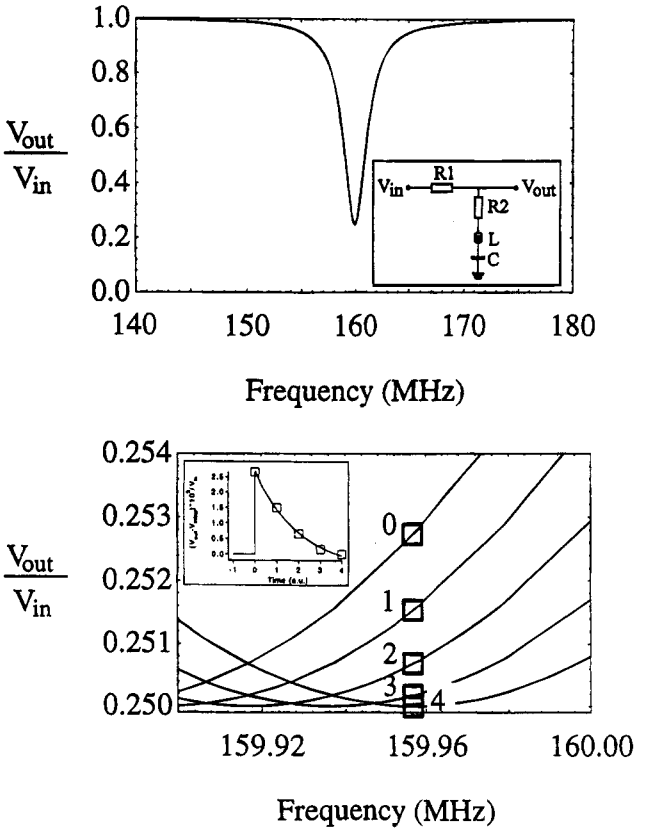

Figure 2. a, top: Q well calculated from eq 1 for the circuit shown in the inset. $R_1 = R_2 = 2\ \Omega$, $L = 240$ nH, $C = 4.125$ pF. b, bottom: Change of Q well due to variation of L and the resulting time-dependent TRRFC signal (inset).

$$\Delta V_{DBM}(t) = V_{DBM}(t) - V_{DBM}(0) = CV_{ref}(V_{out}(t)\cos\delta(t) - V_{out}(0)) \tag{7}$$

using the approximation $\cos\delta \approx 1 - \delta^2/2$ for small δ, eq 7 can be rewritten as eq 8:

$$\Delta V_{DBM}(t) = CV_{ref}\left(V_{out}(t)\left(1 - \frac{\delta^2(t)}{2}\right) - V_{out}(0)\right) \tag{8}$$

Substitution using $\Delta V_{out}(t) = V_{out}(t) - V_{out}(0)$ leads to

$$\Delta V_{DBM}(t) = CV_{ref}\left(-V_{out}(0)\frac{\delta^2(t)}{2} - \Delta V_{out}(t)\frac{\delta^2(t)}{2} + \Delta V_{out}(t)\right) \tag{9}$$

Because the perturbations $\Delta V(t)$ and $\delta(t)$ are small, eq 9 simplifies to

$$\Delta V_{DBM}(t) = CV_{ref}\left(\Delta V_{out}(t) - V_{out}(0)\frac{\delta^2(t)}{2}\right) \tag{10}$$

We note that the phase mismatch yields a voltage decrease whereas the amplitude change yields a voltage increase. Hence, because a voltage increase is observed in our measurements (Figures 3–5), we conclude that the amplitude term dominates and we rewrite eq 10 as follows:

$$\Delta V_{DBM}(t) = CV_{ref}\Delta V_{out}(t) \tag{11}$$

Equation 5 may be used to describe ΔV_{out} in terms of $\Delta L(t)$ and $\Delta R_2(t)$. The former term, $\Delta L(t)$, is believed to be the more important in the present experiment.

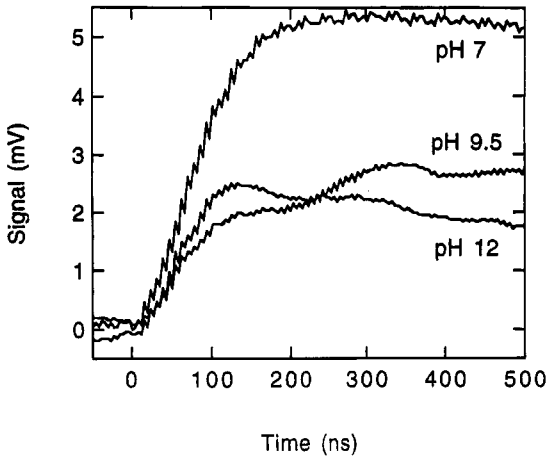

Figure 3. Time resolution and sensitivity of the TRRFC experiment (1 g/L ZnO aqueous suspensions) for pH = 7.0, 9.5, and 12.0. 200 ns/div time base. Overlay of original traces.

Eddy currents may be expressed as a change in the inductance of a unit volume in the center of a solenoid due to a change of the magnetic permeability of the sample:

$$\Delta L = \Delta\mu N/2\sqrt{(r^2 + \lambda^2/4)} \tag{12}$$

where L is the inductance [H], μ is the magnetic permeability [J s^2 C^{-2} m^{-1}], N is the number of turns of the solenoid of radius r [cm], and λ [cm] is the length of the coil.[17] Species with high mobilities within the sample (i.e., charge carriers in the bulk semiconductor or ions in solution) will yield stronger eddy currents and hence larger changes in the inductance of the circuit. The TRRFC experiment is thus most sensitive to semiconductors with charge carriers of high mobilities dispersed in solutions with a low ionic concentration. Ions in the sample solution produce eddy currents which shield the magnetic field and decrease the sensitivity of the apparatus for monitoring charge carrier concentrations by reducing the Q value. The absolute value for the inductance of a solenoidal coil is calculated from eq 13,[18] viz.

$$L = (N^2r^2)/(23r + 25\lambda)\ [\mu H] \tag{13}$$

The resonance frequency f_0 of the tank circuit is given by

$$f_0 = 1/(2\pi(LC)^{1/2}) \tag{14}$$

where C is the capacity of the frequency tuning capacitor.[19]

The time resolution of the TRRFC experiment is limited by the quality (Q) factor of the coil as the response time of the circuit is given by

$$\tau = Q/\pi f_0 = 2L/R \tag{15}$$

where the quality factor Q is given as

$$Q = \frac{1}{R}\sqrt{\frac{L}{C}} = 2\pi f_0 \frac{L}{R} = \frac{f_0}{\Delta f} \tag{16}$$

with R being the real intrinsic resistance of the tank circuit. According to eqs 15 and 16 higher inductivities L (i.e., larger coils) lead not only to an increased sensitivity of the experiment but also to an increase in response times. Various coils have been tested during the present investigations, but best experimental results have been obtained using the coil with the dimensions given earlier.

In summary, the photoinduced generation of additional charge carriers in the sample leads to the generation of eddy currents in the particles from the changing magnetic field in the coil due to the 160 MHz electric field. These currents set up counter magnetic fields which change the inductance of the coil and hence the resonance frequency of the circuit. As a result, RF power is reflected back from the sample circuit to the DBM and the dc output signal increases. As the charge carrier

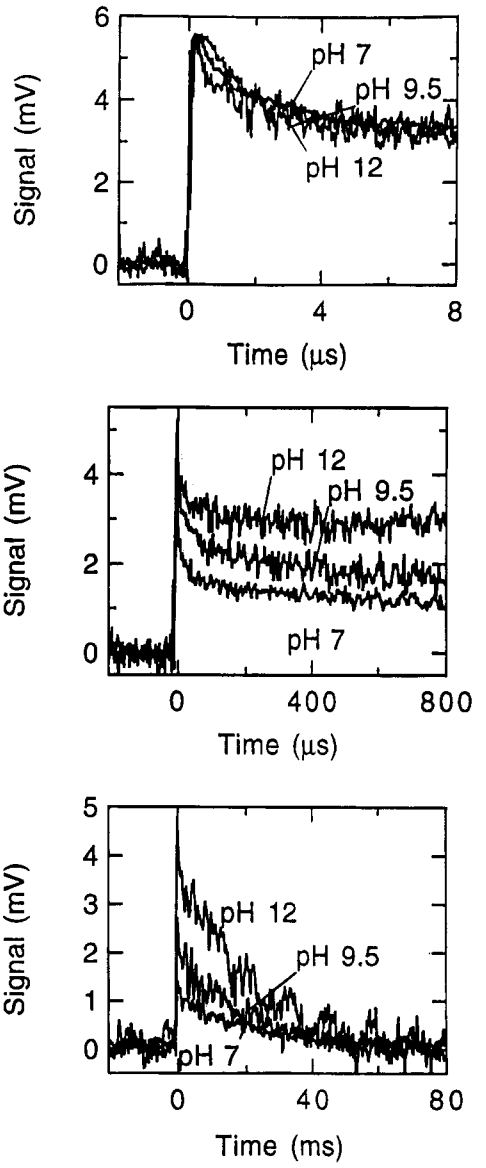

Figure 4. Effect of pH on charge carrier recombination dynamics in 1 g/L ZnO aqueous suspensions. (a, top) 2 μs/div time base, (b, middle) 200 μs/div time base. (c, bottom) 10 ms/div time base, normalized traces (see text).

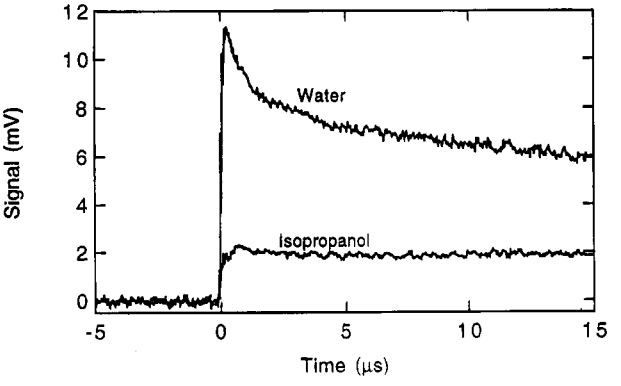

Figure 5. TRRFC signal from 1 g/L ZnO in 2-propanol in comparison to the aqueous suspension at unadjusted pH, i.e., pH = 8.5.

concentration within the sample decays as a function of time, the inductive mismatch between RF bridge and sample decreases, the resonance frequency returns to its initial value, and the DBM produces a smaller dc voltage output. Linearity and sensitivity of the experiments are a function of the shape of the Q well of the circuit. It is assumed for the present investigation that the changes in resonant frequency are small so that the dc output of the DBM is a direct measure for conductivity, i.e., charge carrier concentrations multiplied by their mobilities in the bulk semiconductor medium.

Results and Discussion

Effect of pH. TRRFC traces for samples of 1 g/L ZnO suspended in water at pH = 7.0, 9.5, and 12.0 are shown in Figure 3 for the shortest time scale studied (i.e., up to t = 500 ns after the laser pulse). These unprocessed data show the biggest signals and the slowest time response for pH = 7.0 and the smallest signal with the fastest time response at pH = 12 with the data obtained at pH = 9.5 showing intermediate behavior. This effect is caused by the relative shielding of the ions within the sample solution due to the adjustment of pH. At higher ionic concentration the quality factor of the inductive circuit gets smaller and hence causes faster response times and decreased sensitivity. The data shown in Figure 3 reflect the trends in time resolution, ion content and signal sensitivity as they are expected from the theory of eqs 10−15.

In Figure 4 the data for three longer time scales studied (i.e., 2 μs/div (top), 200 μs/div (middle), and 10 ms/div (bottom)) are shown. The data in Figure 4 have been normalized to identical maximum signal strengths in order to compensate for the effects of ion content of the samples as discussed above. To achieve normalization, the signals taken at pH = 9.5 were multiplied by a factor of 1.41 and those taken at pH = 12.0 by a factor of 2.33. On the shortest time scale (Figure 4a, top) the decay kinetics for charge carrier recombination are identical within experimental error for all three pH values studied.

At the next longer time scales (Figure 4b, middle, in the time domain between 10 μs and 1 ms after laser irridiation), charge carrier concentrations are approximately constant for the sample at pH = 12. Lower pH values lead to increased decay rates for charge-carrier concentration in this time domain. In the experiments with the lowest time resolution applied (Figure 4c, bottom) (i.e., between 1 and 80 ms after photoinjection), the decays of charge carrier concentration are significantly slower for the systems at pH = 12.0 compared to pH = 9.5 or 7.0. Higher pH of the aqueous solutions surrounding the ZnO particles leads to reduced decay rates of the semiconductor charge carriers. This effect is related to a change in the surface speciation of the ZnO particle with changing pH.

The surface of ZnO is amphoteric ($pH_{zpc} = 9.0 \pm 0.3$[11]) and can be described by the following protonation equilibria:

$$>Zn-OH_2^+ \leftrightarrow >Zn-OH + H^+ \quad (17)$$

$$>Zn-OH \leftrightarrow >Zn-O^- + H^+ \quad (18)$$

with $pK_a(17) = 7.6$ and $pK_a(18) = 11.0$.[11] The symbol > denotes a surficial group. At pH 7.0, the principal surface species is $Zn-OH_2^+$, while at pH 9.5 and pH 12.0, Zn−OH and $Zn-O^-$ become the principal surface species, respectively.

The main charge-carrier recombination mechanism, which is proposed based on the data of Figure 3, may be described as follows:

$$>Zn-OH_2^+ + h_{VB}^+ \rightarrow >Zn-OH_2^{2+} \quad (19)$$

$$>Zn-OH + h_{VB}^+ \rightarrow >Zn-OH^+ \quad (20)$$

$$>Zn-O^- + h_{VB}^+ \rightarrow Zn-O \quad (21)$$

Valence-band holes (h_{VB}^+) generated by the photoinjection process are trapped within a time scale of about 100 ns after photoinjection[20,21] by surface hydroxyl groups. Recombination of the charge carriers results from the reaction of conduction-band electrons with the hole traps of eqs 19−21 as follows:

$$\text{pH} = 7.0: \quad >Zn-OH_2^{2+} + e_{CB}^- \rightarrow >Zn-OH_2^+ \quad (22)$$

$$\text{pH} = 9.5: \quad >Zn-OH^+ + e_{CB}^- \rightarrow >Zn-OH \quad (23)$$

$$\text{pH} = 12.0: \quad >Zn-O + e_{CB}^- \rightarrow >Zn-O^- \quad (24)$$

Reactions 22−24 represent the rate-limiting steps in the surface-mediated recombination process. The above mechanism is consistent with experimental findings from recent time-resolved microwave conductivity (TRMC) investigations of TiO_2 photoreactivity.[8,9]

The observed time-dependent decay of the charge-carrier concentration may be characterized kinetically based on the assumption of the above surface-mediated recombination mechanism. We quantify the initial recombination half-lives (Figure 4c) of the orders of magnitude of τ(pH 7.0) $\approx$ 10μs, τ(pH 9.5) $\approx$ 100 μs and of τ(pH 12.0) $\approx$ 10 ms. From these results it appears that the surface speciation of ZnO affects the efficiency of surface-mediated charge carrier recombination. Reactions 20−22 suggest that electrostatic interactions between the surface hole traps and the migrating electrons govern the efficiency of surface mediated recombination of charge carriers. Electron capture by a doubly charged $>Zn-OH_2^{2+}$ surface group (pH = 7.0) is accelerated by Coulombic interactions more than the corresponding reaction of a single positively charged (pH = 9.5) or a neutral surface hole trap group at pH = 12.0. Cross sections for electron capture in semiconductors appear to be correlated with Coulombic repulsion, but no quantitative data are presently available for the three species that characterize the acid−base chemistry of metal oxide surfaces.

Effect of 2-Propanol. To study the effect of added hole scavengers on charge-carrier dynamics, 1 g/L ZnO particles were dispersed in 2-propanol. The resulting TRRFC signal is shown in Figure 5 together with a reference trace obtained in 1 g/L ZnO aqueous suspension without any pH adjustment (pH = 8.5). Figure 5 shows that the charge-carrier concentrations are significantly reduced, and the temporal decay pattern is changed substantially in the presence of 2-propanol. While the TRRFC signal decays in the aqueous system by about 40% in 8 μs, the signal stays nearly constant in the 2-propanol system at a signal level that corresponds to about 20% of the maximum signal in the aqueous suspension. The Q value of the TRRFC apparatus has been found to be constant so that signal strength and temporal behavior of the signals in Figure 5 can be directly compared. The signal obtained in 2-propanol is consistent with a mechanism involving a fast surface reaction of the trapped holes with the solvent (presumably within the electrical double layer surrounding the particles or actually sorbed to the particle surface):

$$>Zn-OH_2^{2+} + (CH_3)_2CHOH \rightarrow >Zn-OH^+ + (CH_3)_2\dot{C}OH + H^+ \quad (25)$$

The electron transfer of eq 25 is most likely completed within the response time of the TRRFC apparatus and thus the rise in signal observed in the 2-propanol experiment at short times is due to the limited time resolution.

As shown above (eqs 22−24), the charge carriers should recombine predominantly via the reaction of surface hole traps with electrons. The relatively slow kinetics of this process in H_2O correspond to the TRRFC signal in Figure 5. From these results we conclude the TRRFC signal, which is detected on the microsecond time scale, arises from the presence of conduction-band electrons because valence-band holes are either trapped at the surface (aqueous system) or have reacted with the organic solvent (2-propanol system). The invariance of the TRRFC signal with time in the microsecond regime may be due to a back-injection of electrons from the 2-propyl radical to the conduction band of ZnO:[22]

$$>Zn-OH_2^+ + (CH_3)_2\dot{C}OH \rightarrow >Zn-OH_2^+ + e^-_{CB} + (CH_3)_2CO + H^+ \quad (26)$$

The smaller TRRFC signal, which is obtained in the 2-propanol experiments, corresponds to a smaller residual concentration of electrons in ZnO. Efficient hole scavenging (e.g., by 2-propanol) yields the accumulation of conduction-band electrons and thus a negative shift in the reduction potential due to charge repulsion.[23] This effect should accelerate the rate of interfacial charge-transfer of conduction-band electrons.[8,24-26] On longer time scales, the TRRFC signals fall to zero in both systems. When the oxidizing capacity of the holes is transferred away from the ZnO particles, electrons are likely to migrate to the ZnO surface, first, and then react with molecular oxygen, which leads to the formation of HO_2/O_2^- and subsequently hydrogen peroxide:[4,11]

$$>Zn-OH_2^+ + e^-_{CB} \rightarrow >Zn-OH_2 \xrightarrow{O_2} >Zn-OH_2^+ + O_2^- \quad (27)$$

followed by

$$O_2^- + H^+ \rightleftharpoons HO_2 \quad (28)$$

and finally

$$2HO_2 \rightarrow H_2O_2 + O_2 \quad (29)$$

Conclusions

The present study establishes the feasibility and potential application of TRRFC to investigate aqueous semiconductor suspensions. High pH conditions lead to extended lifetimes of charge carriers in aqueous ZnO dispersions. However, when 2-propanol is used as a solvent, the charge-carrier dynamics in ZnO appear to be altered completely by the surface reactions of holes with 2-propanol and the back injection of charge carriers into the ZnO conduction band from the 2-propyl radical. In this system, electrons react with dissolved oxygen rather than undergoing surface-mediated recombination with trapped holes as in the case of the aqueous system. The TRRFC method provides a valuable tool for the study of semiconductor conductivity in aqueous semiconductor systems. Future work will concentrate on optimization of sensitivity as well as time resolution of the technique along with investigations with a phase-sensitive detector which may then allow deconvolution of the absorptive and dispersive components leading to the observed TRRFC signals.

Acknowledgment. The authors are grateful for the loan of radiofrequency components from Prof. N.S. Lewis, the help of Prof D. P. Weitekamp's group (especially John Marohn) with radio frequency components, and the use of the excimer laser by Prof. G. A. Blake. Financial support for this project is provided by the Advanced Research Project Agency (ARPA) and the Office of Naval Research (ONR) {NAV 5 HFMNN0001492J1901}. We are grateful to Drs. Ira Skurnick and Harold Guard for their generous support and encouragement. S.T.M. is supported by a National Defense Science and Engineering Graduate Fellowship. H.H. wishes to thank NATO and Deutscher Akademischer Austauschdienst (DAAD) for support. We thank the reviewers of this paper for their stimulating comments.

References and Notes

(1) Hoffmann, M. R.; Martin, S. T.; Choi, W. Y.; Bahnemann, D. W. *Chem. Rev.* **1995**, *95*, 69.
(2) *Photocatalytic Purification of Water and Air*; Ollis, D. F., Al-Ekabi, H., Eds.; Elsevier: Amsterdam, 1993.
(3) Kamat, P. V. *Chem. Rev.* **1993**, *93*, 267.
(4) Hoffman, A. J.; Carraway, E. R.; Hoffmann, M. R. *Environ. Sci. Technol.* **1994**, *28*, 776.
(5) Forbes, M. D. E.; Lewis, N. S. *J. Am. Chem. Soc* **1990**, *112*, 3682.
(6) Kunst, M.; Beck, G. *J. Appl. Phys.* **1986**, *60*, 3558.
(7) Warman, J. M.; deHaas, M. P. *Pulse Radiolysis*, 2nd ed.; CRC Press: Boca Raton, FL, 1991; Chapter 6.
(8) Martin, S. T.; Herrmann, H.; Choi, W.; Hoffmann, M. R. *J. Chem. Soc., Faraday Trans.* **1994**, *90*, 3315.
(9) Martin, S. T.; Herrmann, H.; Hoffmann, M. R. *J. Chem. Soc., Faraday Trans.* **1994**, *90*, 3323.
(10) Lantz, J. M.; Corn, R. M. *J. Phys. Chem.* **1994**, *98*, 9387.
(11) Bahnemann, D. W.; Kormann, C.; Hoffmann, M. R. *J. Phys. Chem.* **1987**, *91*, 3789.
(12) Miller, G. L.; Robinson, D. A. H.; Wiley, J. D. *Rev. Sci. Intrum.* **1976**, *47*, 799.
(13) Yablonowitch, E.; Swanson, R. M.; Eades, W. D.; Weinberger, B. R. *Appl. Phys. Lett.* **1986**, *48*, 245.
(14) Yablonowitch, E.; Allara, D. L.; Chang, C. C.; Gmitter, T.; Bright, T. B. *Phys. Rev. Lett.* **1986**, *57*, 249.
(15) M/A-COM Control Components Division Catalog, 147, Merrimack, NH, 1991.
(16) Warman, J. M.; Schuddeboom, W.; Jonker, S. A.; DeHaas, M. P.; Paddonrow, M. N.; Zachariasse, K. A.; Launav, J. P. *Chem. Phys. Lett.* **1993**, *210*, 397.
(17) Pender, H.; Warren, S. R. *Electric Circuits and Fields*, 1st ed.; McGraw-Hill: New York, 1943; pp 340ff.
(18) Fukushima, E.; Roeder, S. B. W. *Experimental Pulse NMR: A Nuts and Bolts Approach*, 3rd ed.; Addison-Wesley: London, 1980; pp 379, 414.
(19) Thompson, H. A. *Alternating-Current and Transient Circuit Analysis*, 2nd ed.; McGraw-Hill: New York, 1955; pp 143−151.
(20) Rothenberger, G.; Moser, J.; Graetzel, M.; Serpone, N.; Sharmaa, D. K. J. *J. Am. Chem. Soc.* **1985**, *107*, 8054.
(21) Henglein, A. *Ber. Bunsen-Ges. Phys. Chem.* **1982**, *86*, 241.
(22) Hauffe, K. In *Electrochemistry: The Past Thirty and the Next Thirty Years*; Bloom, H., Gutmann, F., Eds.; Plenum Press: New York, 1977.
(23) Brus, L. E. *J. Chem. Phys.* **1984**, *80*, 4403.
(24) Marcus, R. A.; Sutin, N. *Biochim. Biophys. Acta* **1985**, *811*, 265.
(25) Marcus, R. A. *J. Phys. Chem.* **1990**, *94*, 1050.
(26) Lewis, N. S. *Annu. Rev. Phys.* **1991**, *42*, 543.

JP9430587